

Intestinal sodium/glucose cotransporter 3 expression is epithelial and downregulated in obesity

Matúš Soták^{a,b,c,*}, Anna Casselbrant^d, Eva Rath^e, Tamara Zietek^f, Maria Strömstedt^a, Damilola D. Adingupu^a, Daniel Karlsson^a, Maria Fritsch Fredin^a, Peter Ergang^g, Jiří Pácha^g, Anna Batorsky^h, Charles E. Alpers^h, Emma Börgeson^{b,c,i}, Pernille B.L. Hansen^{a,c}, Anette Ericsson^a, Anna Björnson Granqvist^a, Ville Wallenius^d, Lars Fändriks^d, Robert J. Unwin^{a,j}

^a Bioscience, Research and Early Development, Cardiovascular, Renal and Metabolism, BioPharmaceuticals R&D, AstraZeneca, Gothenburg, Sweden

^b Department of Molecular and Clinical Medicine, Wallenberg Laboratory, Institute of Medicine, University of Gothenburg, Sweden

^c Wallenberg Centre for Molecular and Translational Medicine, University of Gothenburg, Sweden

^d Department of Surgery, Institute of Clinical Sciences, Sahlgrenska Academy, University of Gothenburg, Gothenburg, Sweden

^e Chair of Nutrition and Immunology, Technische Universität München, Freising, Germany

^f Department of Nutritional Physiology, Technische Universität München, Freising, Germany

^g Institute of Physiology, Czech Academy of Sciences, Prague, Czech Republic

^h Department of Pathology, University of Washington School of Medicine, Seattle, USA

ⁱ Department of Clinical Physiology, Sahlgrenska University Hospital, Sweden

^j Department of Renal Medicine, Division of Medicine, University College London, UK

ARTICLE INFO

Keywords:

High-fat diet
Leptin deficiency
Obesity
Roux-en-Y gastric bypass
SLC5A4
T2M

ABSTRACT

Aim: We aimed to determine whether the sodium/glucose cotransporter family member SGLT3, a proposed glucose sensor, is expressed in the intestine and/or kidney, and if its expression is altered in mouse models of obesity and in humans before and after weight-loss surgery.

Main methods: We used *in-situ* hybridization and quantitative PCR to determine whether the *Sglt3* isoforms *3a* and *3b* were expressed in the intestine and kidney of C57, leptin-deficient *ob/ob*, and diabetic BTBR *ob/ob* mice. Western blotting and immunohistochemistry were also used to assess SGLT3 protein levels in jejunal biopsies from obese patients before and after weight-loss Roux-en-Y gastric bypass surgery (RYGB), and in lean healthy controls.

Key findings: *Sglt3a/3b* mRNA was detected in the small intestine (duodenum, jejunum and ileum), but not in the large intestine or kidneys of mice. Both isoforms were detected in epithelial cells (confirmed using intestinal organoids). Expression of *Sglt3a/3b* mRNA in duodenum and jejunum was significantly lower in *ob/ob* and BTBR *ob/ob* mice than in normal-weight littermates. Jejunal SGLT3 protein levels in aged obese patients before RYGB were lower than in lean individuals, but substantially upregulated 6 months post-RYGB.

Significance: Our study shows that *Sglt3a/3b* is expressed primarily in epithelial cells of the small intestine in mice. Furthermore, we observed an association between intestinal mRNA *Sglt3a/3b* expression and obesity in mice, and between jejunal SGLT3 protein levels and obesity in humans. Further studies are required to determine the possible role of SGLT3 in obesity.

1. Introduction

Obesity, and associated comorbidities such as cardiovascular disease and diabetes, is a growing health problem worldwide [1]. Impaired

regulation of glucose homeostasis linked to altered intestinal and renal glucose absorption mediated by sodium/glucose cotransporter (SGLT) family members has been suggested as an important component of obesity-related pathophysiology [2,3]. The main role of the SGLTs is

* Corresponding author at: Bioscience, Research and Early Development, Cardiovascular, Renal and Metabolism, BioPharmaceuticals R&D, AstraZeneca, Peparedsleden 1, 431 83 Mölndal, Sweden.

E-mail addresses: matus@sotak.info, matus.sotak@wlab.gu.se (M. Soták).

<https://doi.org/10.1016/j.lfs.2020.118974>

Received 29 September 2020; Received in revised form 11 December 2020; Accepted 20 December 2020

Available online 30 December 2020

0024-3205/© 2021 The Authors. Published by Elsevier Inc. This is an open access article under the CC BY license (<http://creativecommons.org/licenses/by/4.0/>).

thought to be in glucose transport, although important differences exist among the various isoforms. Most recent research has focused on SGLT1 and SGLT2, and SGLT2 inhibitors (e.g., empagliflozin, dapagliflozin, canagliflozin) have been introduced recently as new therapeutic agents, because they can reduce renal glucose reabsorption and help to maintain lower blood glucose levels [4–6], but also have additional cardiovascular and renal benefits [7,8]. SGLT1 is localized predominantly in the intestinal epithelial brush border membrane and has a pivotal role in the absorption of ingested glucose [9]. SGLT1 and other glucose

transporters (GLUT2, GLUT5) are upregulated in intestinal brush border membranes of diabetic patients with hyperglycaemia [2]. Similarly, glucose absorption in the proximal small intestine attributed to SGLT1 is increased in morbidly obese individuals [10]. However, in contrast, hyperleptinemic db/db mice exhibit lower SGLT1 expression, whereas in leptin-deficient ob/ob mice with obesity, SGLT1 expression does not differ from controls [11]. SGLT1 inhibitors or dual SGLT1/2 inhibitors have been under development in preclinical and clinical research [12], but not yet used clinically.

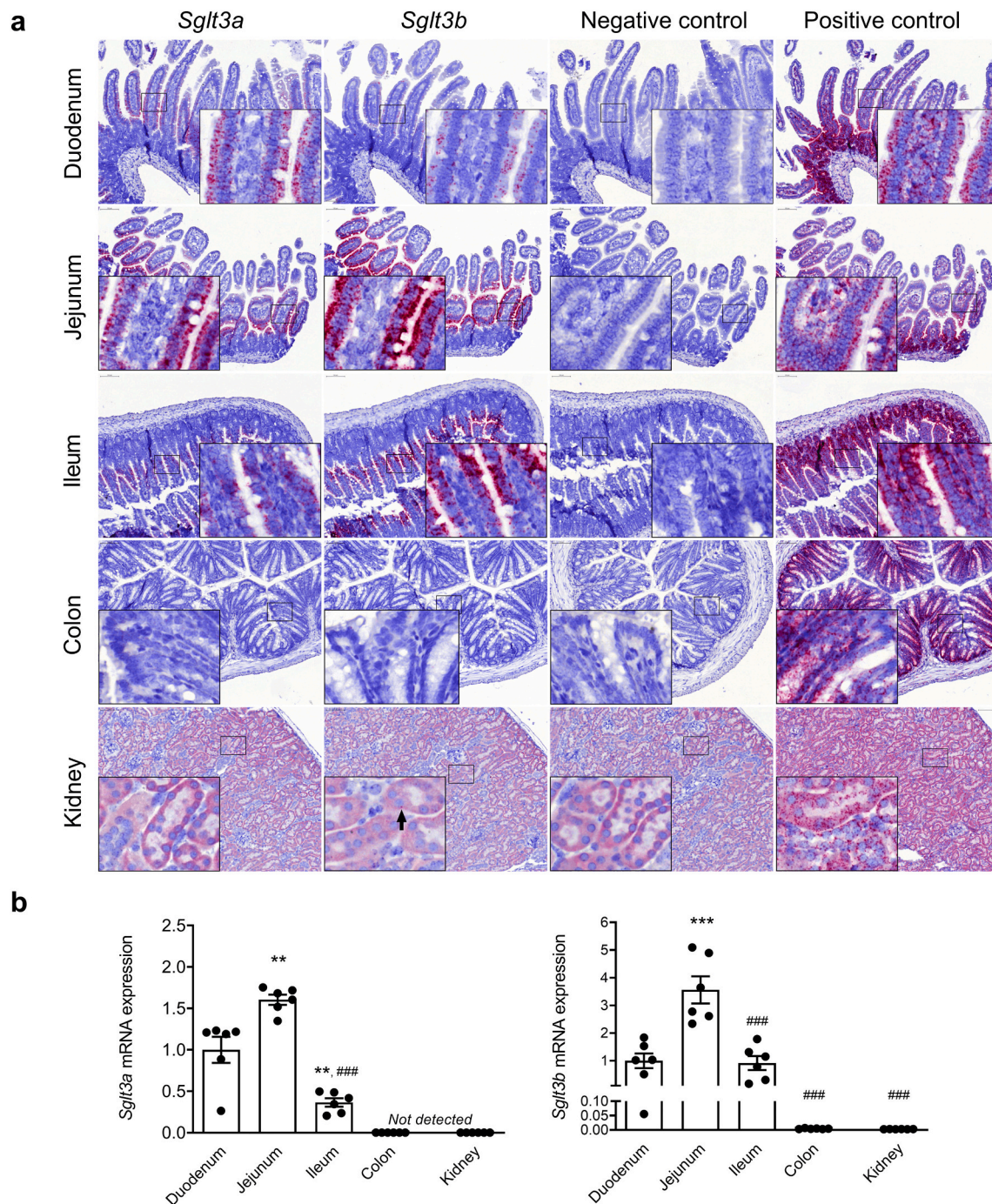


Fig. 1. *Sglt3a* and *Sglt3b* mRNA expression is localized in the epithelium of small intestinal segments in C57BL/6J mice, but absent in the kidney. (a) RNAscope *in-situ* hybridization using mouse *Slc5a4a* (*Sglt3a*), and *Slc5a4b* (*Sglt3b*) anti-sense hybridization probes was performed on paraffin-embedded kidney and intestinal segment tissue sections. Negative control (*B. subtilis* gene *dihydrodipicolinate reductase* anti-sense hybridization), and positive control (*Peptidylprolyl Isomerase B* anti-sense hybridization) is shown for respective organs. The arrow points to positive signal in *Sglt3b* kidney staining. (b) *Sglt3a* and *Sglt3b* mRNA expression was determined by quantitative PCR in matching tissue samples. Data is normalized relative to duodenum and was analysed by one-way ANOVA (Table S1) followed by post-hoc multiple comparisons with Bonferroni correction. ** $P < 0.01$, *** $P < 0.001$ compared with duodenum; ### $P < 0.001$ compared with jejunum.

SGLT3 is a homolog of SGLT1, and despite its recognition over 25 years ago [13,14], very little is known of its physiological function and detailed localisation [15]. However, based largely on *in vitro* data [16,17], it has been proposed to act as a glucose sensor in the gut and/or portal vein [17,18]. In humans, SGLT3 has been putatively localized to submucosal and myenteric neurons of the small intestine, in the kidney, and neuromuscular junction of skeletal muscle [16,19]. Unlike human SGLT3 encoded by *SLC5A4*, there are two rodent isoforms, SGLT3a and SGLT3b, encoded by *Slc5a4a* and *Slc5a4b*, respectively. The localization of the SGLT3a and SGLT3b at the organ level in rodents is thought to be the small intestine and portal vein area, although its more specific localization is unknown [17,18,20]. It is noteworthy that human SGLT3, as well as mouse and rat SGLT3a, do not transport glucose [16,21], but when expressed in oocytes can generate currents with membrane depolarization on exposure to glucose or sodium [16,21]. The currents are larger in an acidic environment, suggesting that SGLT3 activation may

be pH-dependent [16,21]. Although SGLT3 properties have been studied *in vitro*, the detailed localization of SGLT3 and its role in pathophysiology is still lacking.

Thus the aim of this study was to characterize the expression pattern of SGLT3 in the intestine and kidney of mice and to investigate SGLT3 expression in obesity, and to determine if it is affected by gastric bypass surgery-induced weight loss.

2. Results

2.1. Localization of *Sglt3a* and *Sglt3b* mRNA expression in mouse intestinal segments and kidney

The cellular localization of rodent SGLT3 isoforms (SGLT3a coded by *Slc5a4a* and SGLT3b coded by *Slc5a4b*) has not so far been elucidated. Therefore, we used RNAscope *in situ* hybridization to depict mRNA

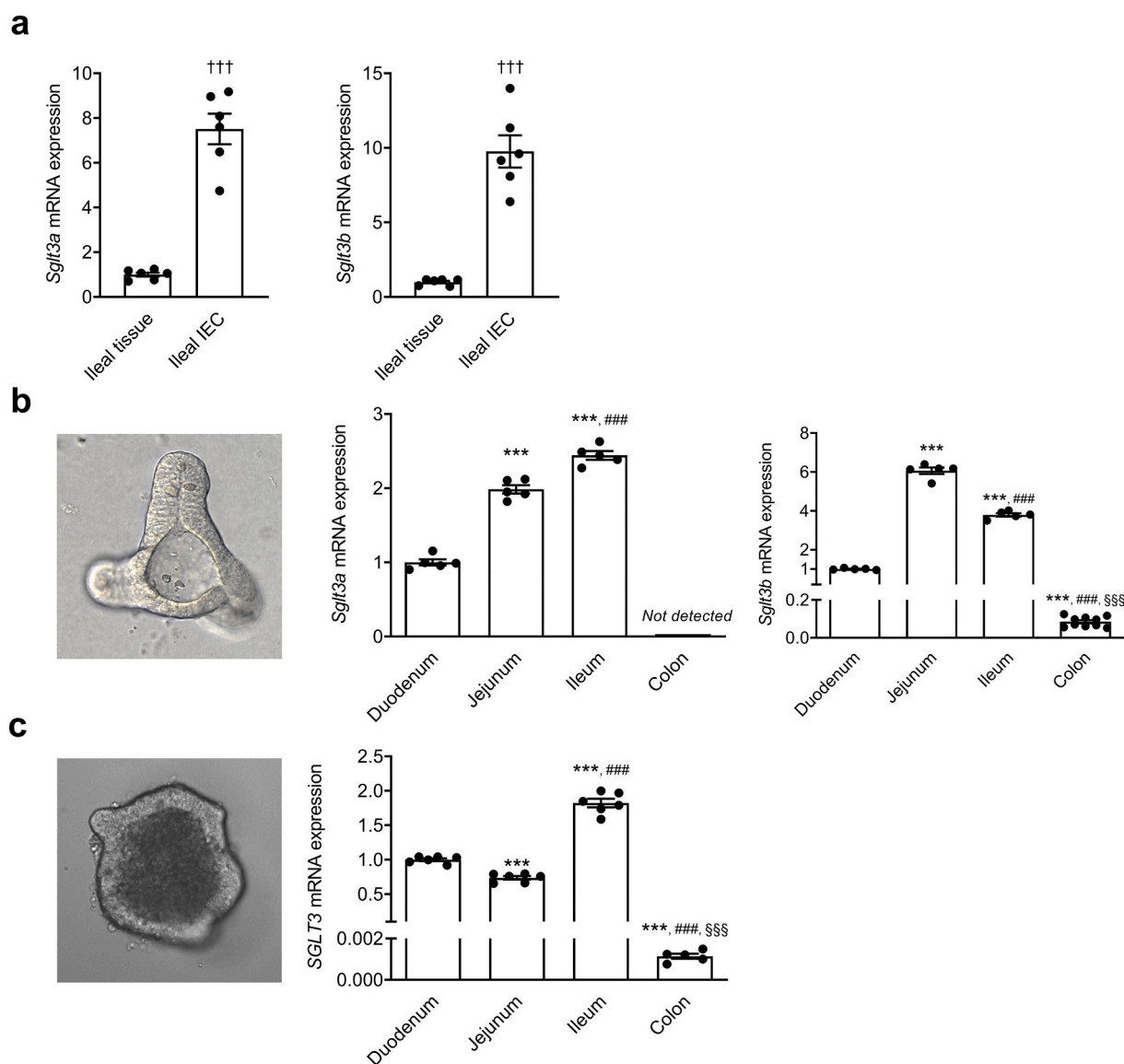


Fig. 2. Confirmed epithelial localization of C57BL/6J mouse *Sglt3a* and *Sglt3b* mRNA expression in isolated intestinal epithelial cells and organoids and human SGLT3 in intestinal organoids, respectively. The mRNA expression of *Sglt3a* and *Sglt3b* in (a) ileum and intestinal epithelial cells isolated from ileum and in (b) intestinal organoids derived from intestinal segments of C57BL/6J mice. (c) Human SGLT3 mRNA expression in organoids derived from crypts of duodenum, jejunum, ileum and colon. The expression was measured by qPCR. Data is normalized relative to ileal tissue (a) or duodenum (b, c) and is presented as individual values and mean \pm SEM. Data was analysed by unpaired Student's *t*-test (a) and one-way ANOVA (Table S1) followed by post-hoc multiple comparisons with Bonferroni correction (b,c), respectively. ^{†††}*P* < 0.001 compared with ileal tissue; ****P* < 0.001 compared with duodenum; ###*P* < 0.001 compared with jejunum; \$\$\$*P* < 0.001 compared with ileum.

distribution along the gastro-intestinal tract and kidney in tissue sections from C57BL/6J mice (Fig. 1a). *Sglt3a* and *Sglt3b* specific hybridization probes clearly indicated expression in all small intestinal segments. Notably, mRNA of both isoforms was localized in the epithelial cells of villi and none was observed in the crypts. The isoform *Sglt3a* did not differ from *Sglt3b* in cellular distribution and both were found in the same locations. However, neither isoform was detectable in the colon. Of note in the kidney, *Sglt3a* expression was undetectable and *Sglt3b* specific hybridization probes gave a very weak signal (Fig. 1a, S1). To confirm the observation made by *in situ* hybridization, we sampled adjacent pieces of intestinal segments used for *in-situ* hybridization and we quantified mRNA expression of *Sglt3a* and *Sglt3b* by qPCR (Fig. 1b). In accordance with *in situ* hybridization, we found the highest expression levels in the jejunum for both *Sglt3a* and *Sglt3b* (Fig. 1b, Table S1). Again, there was little or no expression of *Sglt3a* detected in colon or kidney. In both colon and kidney, *Sglt3b* exhibited lower expression by three orders of magnitude on average compared with the

small intestine, consistent with the results of *in situ* hybridization.

2.2. *Sglt3a*, *Sglt3b* and SGLT3 mRNA expression in intestinal epithelial cells and organoids

To confirm *Sglt3a* and *Sglt3b* localization in epithelia of mouse intestine, we determined mRNA expression in isolated intestinal epithelial cells (IEC) from the ileum. We found significant enrichment of both *Sglt3a* and *Sglt3b* in epithelial cells compared with ileal tissue (Fig. 2a). Furthermore, we assessed the expression in organoids derived from distinct segments of the mouse intestine. Intestinal organoids grown from isolated crypts consist of intestinal epithelial cells and contain all epithelial subpopulations found *in vivo*, with the exception of antigen-presenting M cells that rarely develop without additional supplements in the growth medium [22–24]. We observed similar pattern of the expression along the rostro-caudal gut axis, with the high expression of both *Sglt3a* and *Sglt3b* in the organoids derived from small intestine and

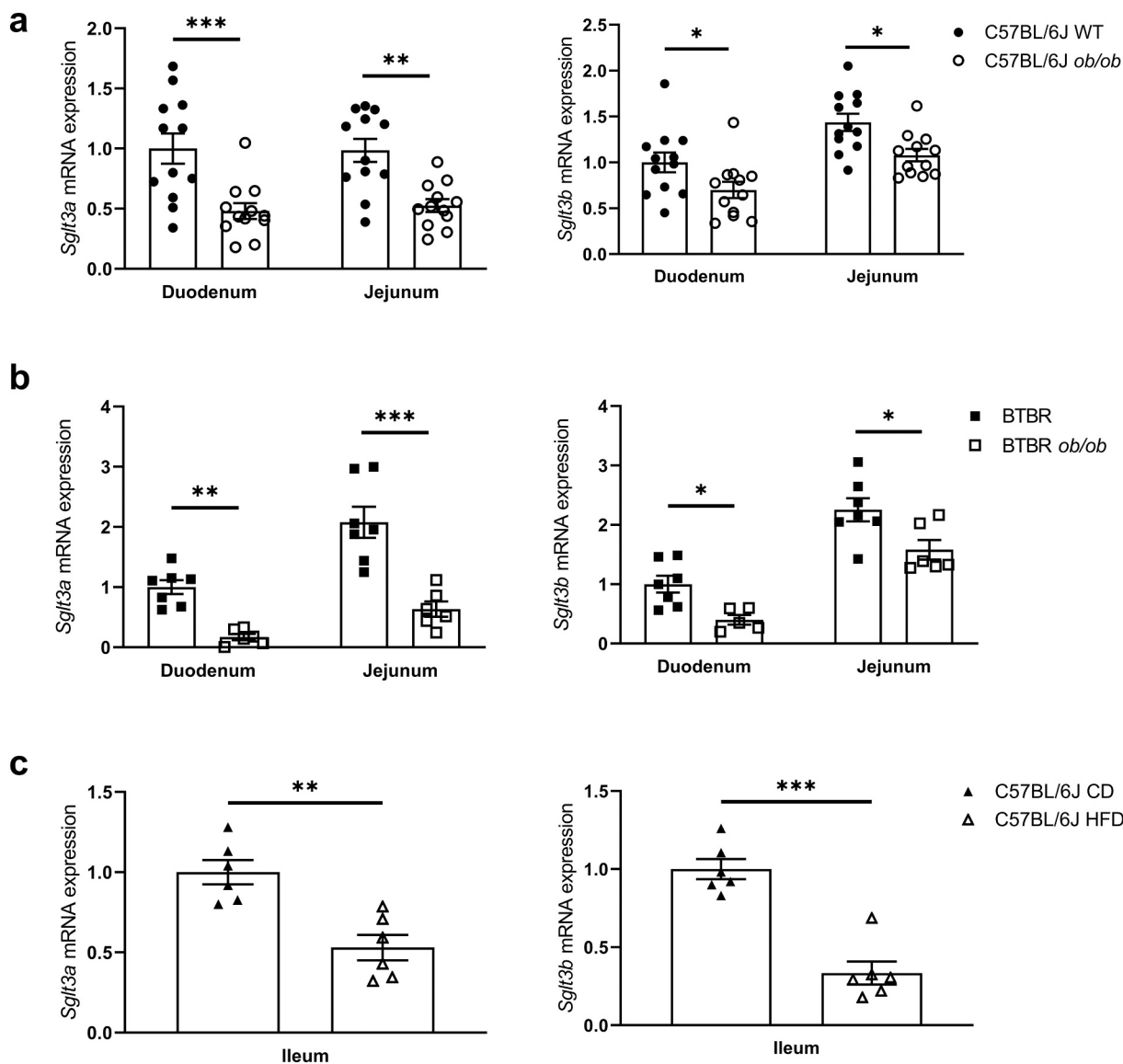


Fig. 3. Obese mice display downregulation of intestinal *Sglt3a* and *Sglt3b* mRNA expression. *Sglt3a* and *Sglt3b* expression was examined either in duodenum and jejunum or ileum of lean and obese mice. Figure (a) shows 21-week old lean C57BL/6J (filled circles) and *ob/ob* (open circles), figure (b) shows 18-week-old BTBR (filled squares) and BTBR*ob/ob* (open squares) mice, and figure (c) shows 16-week-old C57BL/6J mice fed by control diet (CD; filled triangles) or high-fat diet (HFD; open triangles), respectively. The data is normalized relative to duodenum (a, b) or control diet (c) and is presented as individual values and mean \pm SEM. Data was analysed by two-way ANOVA (Table S1) followed by post-hoc multiple comparisons with Bonferroni correction (a, b) or unpaired Student's t-test (c). * $P < 0.05$; ** $P < 0.01$; *** $P < 0.001$.

no or very low expression of *Sglt3a* and *Sglt3b*, respectively, in colon-derived organoids (Fig. 2b, Table S1).

To extend our findings to humans, we determined the expression of *SGLT3* mRNA in organoids derived from intestinal biopsies from patients undergoing surgery. The *SGLT3* expression pattern found in human organoids resembled the mouse situation with dominant expression in the small intestine and almost none detectable in colon

(Fig. 2c, Table S1).

2.3. *Sglt3a* and *Sglt3b* mRNA expression is downregulated in both leptin-deficient and high-fat diet mouse models of obesity

SGLT3 has been proposed to work as an intestinal neuronal glucose sensor and reported previously to be expressed in both intestine and

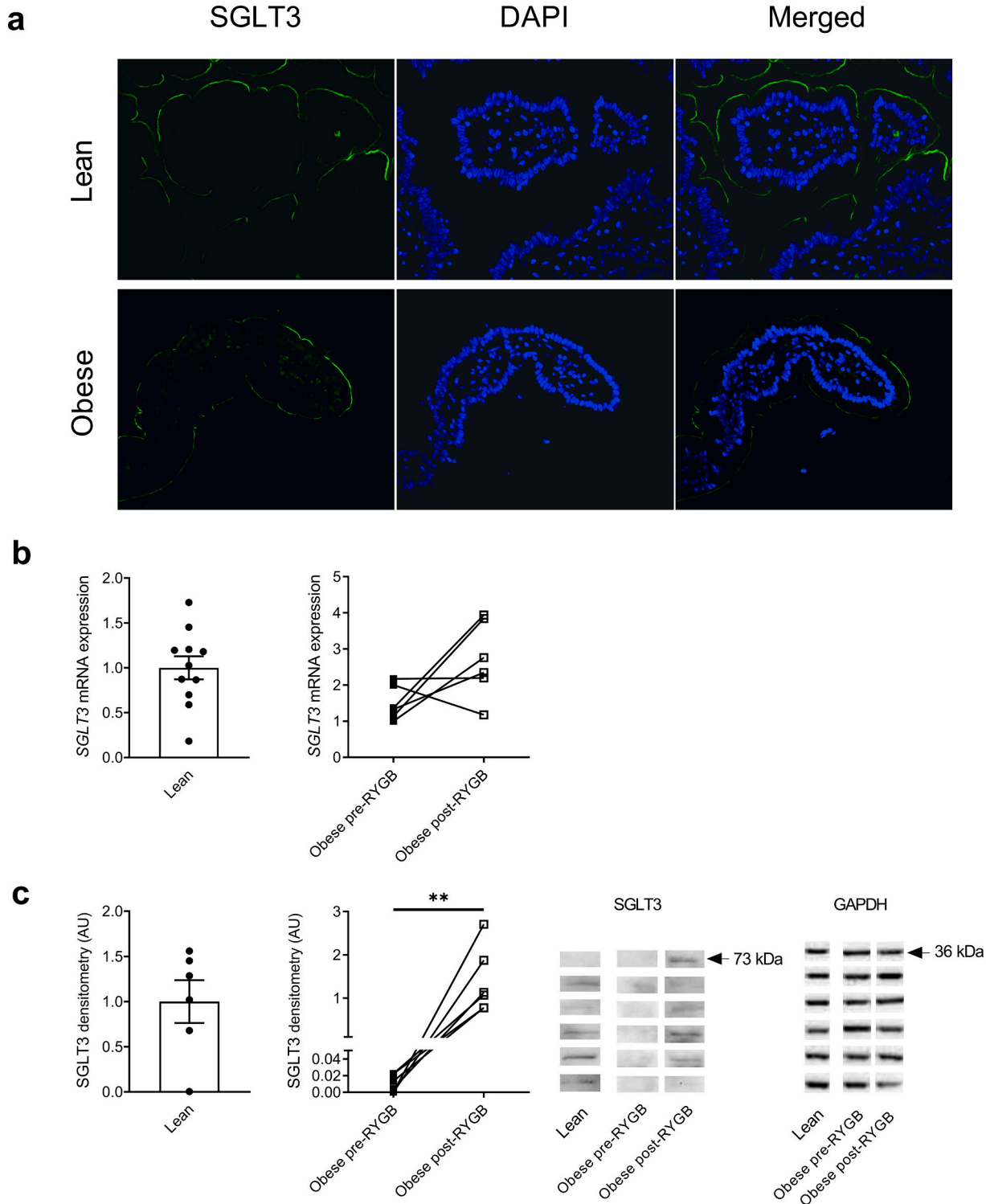


Fig. 4. Intestinal SGLT3 protein is markedly upregulated in obese patients 6 months after Roux-en-Y gastric bypass (RYGB) surgery. (a) SGLT3 protein localize to jejunum epithelium of healthy and obese individuals. (b) qPCR and (c) Western blot analysis of jejunal biopsies from healthy volunteers and from obese patients before and 6 months after bariatric surgery. Data is normalized relative to mean of lean controls. Data was analysed by two-tailed paired t-test. **P < 0.01.

kidney [16,19]; however, its expression pattern has also not been characterized in disease. Since altered glucose sensing might play a role in obesity and associated pathologies, we determined the mRNA expression of mouse *Sglt3a* and *Sglt3b* in small intestine (duodenum and jejunum) and kidney using qPCR in two types of leptin-deficient mouse models with different weight gain (Fig. S2a, [25]), and in ileum of a high-fat diet-induced obesity model (Fig. 3).

Sglt3a and *Sglt3b* were downregulated in the duodenum and jejunum of obese *ob/ob* mice compared with their lean littermates (Fig. 3a, Table S1). *Sglt3a* mRNA expression was again undetectable and the expression of *Sglt3b* mRNA 4 orders of magnitude lower in the kidney compared with the small intestine (data not shown).

In *BTBRob/ob* mice we observed downregulation of both *Sglt3a* and *Sglt3b* in the duodenum and jejunum compared with lean littermates (Fig. 3b, Table S1). Similar to *ob/ob* mice, the *BTBRob/ob* strain displayed no *Sglt3a* and only very low levels of *Sglt3b* renal expression (data not shown).

We also found similar downregulation of both *Sglt3a* and *Sglt3b* mRNA expression in the ileum of high-fat diet-fed (HFD) mice (Fig. 3c).

2.4. Obesity-induced downregulation of intestinal epithelial SGLT3 is restored by surgery-induced weight loss

To correlate our findings from the mouse models to human obesity, we examined SGLT3 mRNA and protein expression in intestinal biopsies obtained from obese individuals undergoing RYGB surgery and young lean volunteers. By immunofluorescence staining, we identified SGLT3 localization mainly in the epithelial brush border membrane (Fig. 4a) in the biopsies from both lean and obese individuals. Although *SGLT3* mRNA expression was not significantly different (Fig. 4b), SGLT3 protein assessed by Western blotting was substantially upregulated by RYGB-induced weight loss in obese patients (Fig. 4c, Fig. S3). SGLT3 mRNA and protein were detected in lean individuals and the level were similar to both pre- and post-surgery obese groups or to post-surgery obese patients, respectively. (Fig. 4b, c).

3. Discussion

SGLT3 was originally proposed as a glucose sensor [16,26] present in human submucosal and myenteric neurons, as well as in the neuromuscular junctions of skeletal muscle [16]. Diez-Sampedro and colleagues [16] used confocal microscopy to demonstrate co-localization of SGLT3 and acetylcholine receptor β -subunit in human small intestine and in skeletal muscle biopsies. However, in contrast, although we cannot exclude neuronal expression, we found intestinal expression of SGLT3 to be consistently localized to the epithelium, and highly expressed in the small intestine, though absent in the colon. Previous studies have also reported that SGLT3 is present in kidney [19], but we were unable to confirm this. Indeed, our data in mouse and human tissue samples, mouse IEC, and in intestinal organoids derived from both species, clearly show epithelial expression in enterocytes. Transcriptional profiling of both enteroendocrine cell and enterocyte populations has also detected *SGLT3* mRNA [27,28], as well as its expression in the Caco2 cell line [29], which although originally derived from a human colon cancer has many of the transport characteristics of small intestinal epithelia, and *SGLT3b* has also been detected in mouse intestinal brush-border membrane proteins [30]. Based on the similarity in the functional properties studied in oocytes *in vitro* [16,21,31] and the expression patterns in mouse and human organoids, it seems that although both rodent isoforms share some aspects of its human single homolog SGLT3, it is SGLT3a isoform that resemble human SGLT3 more than the SGLT3b [15]. All in all, SGLT3 expression appears to be consistently and predominantly localized to the intestinal epithelium.

Interestingly, α -glucosidase inhibitors like 1-deoxynojirimycin and miglitol are potent SGLT3 agonists [32]. Primarily, they inhibit intestinal glucose absorption [33], by delaying disaccharide digestion.

However, it might be possible that a direct agonistic effect of miglitol on SGLT3 could contribute to reduced glucose absorption, since miglitol has been shown to act on SGLT3 to activate Ca^{2+} /calmodulin-dependent protein kinase II in duodenal enteroendocrine cells [20]. Thus, our finding of SGLT3 epithelial expression, which contradicts earlier reported neuronal localization, may still be consistent with the hypothesis that SGLT3 is a glucose sensor, perhaps involved in incretin secretion [20,34]. This function would require epithelial localization to sense luminal glucose; *SGLT3* mRNA has been detected in small intestinal enteroendocrine cells, although at a level not dissimilar to enterocytes, and does not seem to be enriched in enteroendocrine cells [28]. It may also be relevant that we found the highest expression of SGLT3 in earlier parts of the small intestine, where a lower pH could enhance SGLT3 stimulation [16,21]. Considering that SGLT3 does not transport glucose, but transports sodium ions [19] in the presence of glucose and low pH [16], activation would be expected to reduce the driving force for SGLT1 glucose uptake in more proximal parts of the small intestine, resulting in greater distal delivery of glucose to act on endocrine cells and thereby increase stimulation of GLP-1 secretion [35]. Interestingly, SGLT3 can also elicit currents in the absence of Na^+ and transport H^+ in the presence of glucose [16,21]. We could speculate that this would enable to sense the chyme coming from stomach to intestinal parts even in the absence of Na^+ . Indeed, the role of SGLT3 in regulation of gastric emptying has been suggested based on indirect evidence [36], but we were not able to confirm this effect using miglitol as SGLT3 agonist in rats *in vivo* (Soták et al., unpublished data). Moreover, we could speculate that proton-generated currents in the presence of glucose could be relevant in the activation of enteroendocrine cells by SGLT1-independent mechanism or release of secretin, which is activated by low pH [37]; however, these hypotheses need to be tested.

Based on the original glucose sensing concept, we speculated that SGLT3's expression pattern may be altered in obesity. To investigate this, we examined SGLT3 expression in experimental mouse models of genetically-induced obesity and type 2 diabetes (C57BL/6J *ob/ob* and *BTBRob/ob* with higher weight gain; Fig. S2a, b), and high-fat diet-induced obesity with glucose intolerance (Fig. S2c, d). We found that the intestinal expression of SGLT3 is significantly downregulated in obese mice. We then extended our observations from experimental animal models to human pathophysiology, confirming that SGLT3 is expressed in normal human intestinal epithelium and that it is substantially upregulated by RYGB-induced weight loss. SGLT3 detected in obese patients appeared to be lower compared with lean individuals, but a limitation of our patient cohort is that it is not age- and sex- matched, so we cannot exclude any effect of age or sex.

Hyperglycaemia might contribute to the lower SGLT3 expression, but does not seem to be essential for the effect, since the downregulation is observed not only in hyperglycaemic genetically-determined obese mice (Fig. S2b), but also in diet-induced obesity, where the mice are only slightly hyperglycaemic (Fig. S2c). No meaningful correlation between HbA1c and *Sglt3* expression was detected (data not shown). The abundance of glucose transporters is subjected to a complex regulation on the level of transcription, mRNA stability, translation/protein stability, and protein trafficking. For SGLT1, it is known that luminal glucose can regulate expression at the post-transcriptional and post-translational levels, but not necessarily at the mRNA level [38]. As it seems that *ob/ob* mice show a downregulation of *Sglt3* independent of diet (both WT and *ob/ob* were kept on R3 chow diet), luminal glucose does seem to be the driving force. Leptin was also shown to downregulate expression of *Sglt1* [39]. However, at the same time we observed downregulation in hypoleptinemic mice (*ob/ob*) and potentially hyperleptinemic obese patients, and so it does not seem likely that leptin is the main regulator of SGLT3. However, the degree of fat mass might be a driver, since most pronounced *Sglt3* downregulation was observed in *BTBR ob/ob* mice that gained a higher amount of weight (Fig. S2a, [25]). Adipokines produced by adipose tissue have already been shown to impact IEC homeostasis [40], although HFD mice gained only a little weight and

still showed the same phenotype regarding SGLT3 expression.

Downregulation of SGLT3 in obesity in the context of increased SGLT1-mediated glucose uptake [2,10] may lead to a reduced GLP-1 response [41] that is restored in patients following gastric bypass surgery and weight loss. Indeed, both GLP-1 levels [42] and GLP-1 producing enteroendocrine cells in Roux limb [43] are significantly increased in patients following RYGB. A role in epithelial remodelling and heightened sweet taste perception following RYGB has also been proposed [18,44,45]. Bhutta et al. detected higher SGLT3b mRNA expression in the common limb compared with the biliopancreatic or Roux limbs in a rat RYGB model [44]. However, they did not provide a comparison with the sham-operated rats and it cannot be concluded whether RYGB caused the observed changes or if such regional differences are also present in intact rats. In our patients we collected tissue from the Roux limb, but we cannot exclude that the changes after RYGB also occur in the common limb.

In contrast to our observation of upregulated SGLT3 after RYGB, Ren et al. [46] reported downregulation of SGLT3 expression in a mouse model of sleeve gastrectomy (VSG). There are several important differences between our study and theirs. While their data were observed in wild type C57BL/6J mice on a standard diet, we report findings in obesity in humans, the condition for which VSG and RYGB are carried out in clinical practice. Substantial differences between RYGB and VSG have also been reported: hyperplasia and increase in both villus height and crypt depth have been observed after RYGB [43,47], but not following VSG [43,48]; the increased number of GLP-1 positive cells was detected after RYGB and 14-days post-VSG [43], but not 3-months after VSG [48]; glucose transporters GLUT1/2/5 and SGLT1 were overexpressed in RYGB and associated with increased glucose disposal, but no changes in expression of these transporters were observed in VSG, in which glucose absorption is delayed [43,49]. Thus, it seems likely that SGLT3 may be differentially regulated following different forms of weight loss surgery. The present findings contribute to our knowledge of post-RYGB changes in Roux limb-related glucose sensing, uptake, and homeostasis [50,51], and provide a potentially novel target of interest for future study.

Finally, mouse intestinal *Sglt3a* mRNA has been reported to exhibit diurnal variation and regulated by a circadian clock [52]. We confirmed circadian rhythm of *Sglt3a* mRNA in Wistar rat small intestine (Soták et al., unpublished data; [53]). This is in accordance with hypotheses of SGLT3 role in glucose sensing or sodium absorption, since both glucose absorption [54] and sodium absorption [55] show rhythmic pattern, too. Impaired peripheral clock and rhythmic locomotor activity have been reported in *ob/ob* mice and shown to precede the development of metabolic abnormalities [56]. High-fat, high-sucrose diet altered the rhythmic secretion of GLP-1 in rats [57]. Thus, *Sglt3* downregulation observed in our *ob/ob* and HFD mouse models might be related to peripheral circadian clock impairment. Circadian variation throughout the 24 h also needs to be taken into consideration when designing experiments of diurnally regulated targets including SGLT1 and SGLT3 [52,58].

4. Conclusions

In conclusion, we report that *Sglt3a/Sglt3b* mRNA expression, and mRNA and protein expression of SGLT3, appear to be located almost exclusively to the intestinal epithelium in mice and humans, respectively. We also found no evidence for significant renal expression of SGLT3. We have shown that *Sglt3a/Sglt3b* mRNA expression is altered in experimental mouse models of obesity and that low SGLT3 protein expression detected in morbidly obese humans is upregulated following RYGB-induced weight loss. However, while these original, though descriptive, changes in SGLT3 expression observed in our mouse models and in obese patients are broadly consistent and intriguing, their true functional significance remains to be elucidated.

5. Materials and methods

5.1. Mice

C57BL/6J male mice ($n = 5$) were obtained from AstraZeneca animal breeding facility (Gothenburg, Sweden) and sacrificed at the age of 14 weeks. B6.Cg-*Lep^{ob}/J* male mice (*ob/ob*, $n = 12$) and respective lean control littermates (*ob/+*, $n = 12$) were purchased from The Jackson Laboratory (stock no. 000632, Bar Harbor, ME, US) at 6 weeks of age, acclimatized and sacrificed at 21 weeks of age. The mice were also utilized in another study [59]. BTBR.Cg-*Lep^{ob}/WiscJ* female mice (BTBR*ob/ob*, $n = 6$) and their respective lean littermates (BTBR, $n = 7$) were purchased from The Jackson Laboratory (stock no. 004824), acclimatized and sacrificed at 18 weeks of age. All animals were maintained at 12:12 h light-dark regime in enriched environment with *ad libitum* access to standard chow diet (R3, Lantmännen, Stockholm, Sweden) and drinking water throughout the study.

Mice were anesthetized using 5% isoflurane and euthanized by exsanguination. Kidneys and two adjacent intestinal segments 2 cm in length were collected for *in situ* hybridization and RNA analysis, respectively, from 14-week-old C57BL/6J mice. Specifically, duodenum was collected 1 cm distally of the stomach, jejunum was collected at the midline of the small intestine, ileum was collected 1 cm proximally from the caecum, and colon was collected at midline between caecum and rectum. The samples for *in situ* hybridization were placed in 4% paraformaldehyde. Mucosal scrapings of intestinal segments of duodenum (defined as 6 cm proximal segment 1 cm distally from stomach), and jejunum (defined as 6 cm segment in the middle of small intestine) were collected from obese mice and their littermates. Kidneys were harvested and divided by a sagittal section. All samples collected for subsequent RNA isolation were immediately snap-frozen in liquid nitrogen and stored at $-80\text{ }^{\circ}\text{C}$.

C57BL/6J mice received pelleted chow food (*M/Z* autoclavable V1124-3, Ssniff, Soest, Germany) and water *ad libitum*. At the age of 8 weeks, mice were switched to control diet (CD) for 4 weeks: 13 kJ% fat based on soy oil, (S5745-E702; Ssniff, Soest, Germany). Subsequently, mice were fed CD or a plant-based high-fat diet (HFD) with 48 kJ% of fat (S5745-E712; Ssniff, Soest, Germany) for 4 weeks [60]. Ileal tissue as well as ileal intestinal epithelial cells were isolated from mice on control diet as described previously [61]. For organoid preparation, chow-fed C57BL/6J mice at 8–18 weeks of age were used [22]. C57BL/6J mice used for diet-induced obesity and organoid preparation were bred and kept in the animal facility of the Institute for Food & Health (ZIEL, Freising, Germany).

Animal care and experiments were performed in accordance with the Directive 2010/63/EU of the European Parliament on the protection of animals used for scientific purposes, and was approved by The Regional Animal Ethics Committee for Experimental Animals, University of Gothenburg or Bavarian Animal Care and Use Committee, respectively.

5.2. *In situ* hybridization

Intestinal segments (duodenum, jejunum, ileum, colon) and kidneys from 5 mice were fixed in 4% paraformaldehyde for 24 h and dehydrated in subsequent ethanol washes followed by paraffin embedding. Subsequently, transversal intestinal sections and sagittal kidney sections were prepared from paraffin blocks and placed on Superfrost Plus histological slides (Thermo Fisher Scientific, Waltham, MA). To detect mRNA localization in mouse intestine and kidney tissue samples, we performed *in situ* hybridization using RNAscope 2.5 High Definition — Red Assay (Advanced Cell Diagnostics, ACD, Newark, CA) according to the manufacturer's instructions. Briefly, the slides were baked in a dry oven for 1 h at $60\text{ }^{\circ}\text{C}$ and deparaffinised in multiple xylene and 100% ethanol wash at room temperature (RT). RNAscope Hydrogen Peroxide was applied for 10 min at RT followed by target retrieval for 15 min at $95\text{ }^{\circ}\text{C}$ in RNAscope 1 × Target Retrieval Reagent and protease incubation

in RNAscope Protease Plus for 30 min at 40 °C. The slides were washed in 1 × RNAscope Wash buffer and incubated with specific mouse *Slc5a4a* (cat. no. 462281), *Slc5a4b* (cat. no. 468891), positive control *Ppib* (cat. no. 313911) and negative control bacterial *dapB* (cat. no. 310043) hybridization probes for 2 h at 40 °C. Subsequent incubations were performed with AMP1–6 reagents (RNAscope 2.5 HD Red Reagent Kit, ACD, cat. no. 322350) followed by incubation with detecting RED solution (1:60 ratio of Fast RED-B to Fast RED-A). The slides were subsequently counterstained with 50% Haematoxylin, dried at 60 °C for 15 min and mounted using EcoMount medium. The slides were evaluated by histologist and analysed by semi-quantitative scoring.

5.3. RNA isolation, cDNA synthesis and quantitative PCR

Frozen tissue was homogenized in RLT buffer (Qiagen, Hilden, Germany) and total RNA was isolated using RNeasy Mini Kit (Qiagen) with on-column DNase I treatment using automated sample preparation on QIAcube instrument (Qiagen). The purity and quantity of RNA was assessed using Nanodrop Spectrophotometer (Thermo Fisher Scientific). First strand cDNA was synthesized from 1 µg of template RNA using random primers and High-Capacity cDNA Reverse Transcription Kit (Thermo Fisher Scientific) according to the manufacturer's instructions. Quantitative real-time PCR was performed on 5 times diluted cDNA using specific TaqMan Gene Expression Assays (*Slc5a4a*, assay ID: Mm01173149_m1; *Slc5a4b*, assay ID: Mm00452283_m1; *Hprt*, assay ID: Mm00446968_m1) and TaqMan Gene Expression Master Mix (Thermo Fisher Scientific). The PCR reactions were performed in triplicates using QuantStudio 7 Flex Real-Time PCR System (Thermo Fisher Scientific) according to the manufacturer's instructions. C_t values were obtained for target genes and normalization gene using automatic threshold detection, and C_t values <35 were considered acceptable for quantification. Quantification was performed using the standard calibration curve and *Hprt* as the normalization gene, which was stable across the experimental groups. Data in the figures are presented as expression levels relative to the duodenum (Fig. 1b, 2b, c, 3a, b), to the ileal tissue (Fig. 2a), control diet (Fig. 3c) or lean subjects (Fig. 4b, c).

5.4. Organoid generation and harvesting

Human intestinal organoids were derived from macroscopically healthy tissue of surgical specimen. The study procedures were performed in accordance with the Declaration of Helsinki and approved by Regional Ethical Review Board; all participants in this study gave their written informed consent. Mouse [22] and human [62] intestinal organoids from duodenum, jejunum, ileum and colon were prepared and cultured as previously described. Briefly, Matrigel containing crypts/organoids were plated. After polymerization at 37 °C, 300 µL of crypt culture medium containing growth factors (EGF, R-Spondin 1, Noggin) was added to mouse small intestinal organoids, medium for mouse large intestinal organoids was furthermore supplemented with WNT3. Medium for human intestinal organoids contained EGF, R-Spondin 1, Noggin, WNT3A, A83–01, and SB202190. After 7 days (mouse) and 10 days (human), respectively, organoid cultures were passaged and harvested after two passages. Total RNA isolation, reverse transcription and quantitative PCR were performed as reported previously [22] with probes and primers specific for mouse *Slc5a4a* and *Slc5a4b* genes and human *SLC5A4* gene.

5.5. Subjects and tissue samples

Patients waiting for Roux-en-Y gastric bypass surgery (RYGB) and healthy volunteers, respectively, willing to participate gave their written consent and were enrolled in the study. The study procedures were performed in accordance with the Declaration of Helsinki and approved by Regional Ethical Review Board in Gothenburg (ethical approval No: 007–09 and 001–11). Patients scheduled for RYGB (5 women, 1 man;

mean age 52.3 years (range 43–60), mean BMI 39.7 (range 37–43)) at Sahlgrenska University Hospital underwent an upper-gastrointestinal endoscopy before starting on a pre-operative very low-calorie diet (900 kcal/day). Biopsies were retrieved approximately 50 cm distal to ligament of Treitz. Between six to eight months after surgery the patients (mean BMI 31.1 (range 29–36)) underwent a new endoscopic examination of the Roux limb.

Jejunal biopsies were also collected from healthy volunteers (6 men; mean age 25.8 (range 24–30), mean BMI 22.6 (range 19–25)) approximately 50 cm distal to the ligament of Treitz. All specimens were immediately snap-frozen in liquid nitrogen for Western blot analysis or fixed in 4% formaldehyde for immunohistochemistry analysis. Characteristics of volunteers and patients are summarised in Table S2.

5.6. Immunofluorescence staining of human samples

Fixed jejunal samples were embedded in paraffin. Sections (3 µm) were mounted on slides, deparaffinised and boiled in 10 mM citrate buffer (pH 6.0) containing 0.05% TWEEN-20 (Sigma-Aldrich, Stockholm, Sweden) for 20 min and left to cool for 2 h to retrieve antigens. Samples were then incubated for 2 h in blocking solution (5% goat-serum in PBS containing 0.3% Triton-X-100, Sigma-Aldrich) and afterwards incubated overnight with the primary SGLT3 antibody (Antibody registry ID: AB_2650519; cat. no. 24327-1-AP, Proteintech, Manchester, UK). After washing (PBS containing 0.3% Triton-X-100) the slides were incubated with secondary goat-anti rabbit Alexa Fluor488 antibody (Invitrogen, Carlsbad, CA) for 2 h. The complex was stained with Hoechst stain solution (Sigma-Aldrich) and mounted with anti-fade water-soluble medium (Sigma-Aldrich). Protein was detected by Nikon Eclipse E400 (Nikon, Tokyo, Japan) using the DAPI (340–380 nm) and FITC (465–495 nm) filters and ACT-1 software (Nikon).

5.7. Quantitative PCR and Western blot analyses of human intestinal mucosa

Biopsy tissue specimens were homogenized in RNA-STAT 60 reagent (AMS Biotechnology, Abingdon, UK) and RNA isolated using RNeasy Mini kit (Qiagen) followed by DNase I (Invitrogen) treatment and cDNA synthesis (SuperScript IV, Invitrogen). Quantitative PCR was performed using HOT FIREPol Probe qPCR Mix Plus with ROX (Solis BioDyne, Tartu, Estonia) and respective assay (*SLC5A4*: Hs00429527_m1, *LRP10*: Hs01047362_m1, *RPLP0*: 4326314E, 18S rRNA: 4319413E; Thermo Fisher Scientific). Data were normalized to geometric mean of three endogenous controls (*LRP10*, *RPLP0*, 18S rRNA). Western blot analysis was performed as described previously [63]. Briefly, specimens were homogenized in a PE buffer (10 mM potassium phosphate buffer, pH 6.8 and 1 mM EDTA) containing 10 mM 3-[(3-cholamidopropyl)dimethylammonio]-1-propane sulphate (CHAPS, Boehringer Mannheim, Mannheim, Germany) and protease inhibitor cocktail (Roche Diagnostics, Stockholm, Sweden). Samples diluted in SDS buffer were loaded on a NuPage 10% Bis-Tris gel in MOPS buffer (Invitrogen). The proteins separated by electrophoresis were transferred to a polyvinylidene difluoride transfer membrane (Amersham Hybond, 0.45 µm, RPN303F, GE Healthcare, PA) using the iBlot dry blotting system (Invitrogen). The membranes were washed and blocked in 0.2% (w/v) I-block reagent (Applied Biosystems, Waltham, MA) at RT before incubation with primary antibody against SGLT3 (RRID:AB_2650519, cat. 24327-1-AP, Proteintech) and the loading control glyceraldehyde-3-phosphate dehydrogenase (GAPDH, RRID:AB_613387, cat. IMG-5143A, Imgenex, San Diego, CA) overnight at 4 °C. HRP-conjugated secondary antibody (#7074, Cell Signaling Technology, Danvers, MA) was applied for 1 h at RT and visualized using the WesternBright Quantum reagents (K-12042, Advanta Corporation, Menlo Park, CA). The intensities of specific bands were detected using a ChemiDoc XRS camera and analysed by Quantity One software (Bio-Rad Laboratories, Hercules, CA). The optical density of SGLT3/GAPDH represents the

result. The first antibody was removed by stripping buffer (Re-Blot Plus Mild Solution, Millipore, Temecula, CA) before the next antibody was used.

5.8. Statistical analysis

The data are presented as individual and mean values \pm SEM (standard error of the mean). To assess differential expression, Gaussian distribution was assumed based on Q-Q plots and one-way or two-way ANOVA was applied followed by post-hoc comparisons with Bonferroni correction using GraphPad Prism 8.3 (GraphPad Software, San Diego, CA, USA). In case of two independent or dependent groups, unpaired two-tailed Student's *t*-test or paired *t*-test was applied, respectively. *P* < 0.05 was considered statistically significant.

CRediT authorship contribution statement

R.J.U. conceived the project. M.So., and R.J.U. conceptualized and designed the study, in consultation with A.E., P.B.L.H., A.B.G., L.F., T.Z., J.P., C.E.A. Sample collection, experimental procedures and statistical analysis of data was done by M.So., A.C., E.R., T.Z., M.St., D.D.A., D.K., M.F.F., P.E., A.B., A.E., A.B.G., V.W. All authors interpreted the data. M. So., E.B., C.E.A., R.J.U. wrote the paper. All authors revised and commented on the manuscript.

Declaration of competing interest

M.St., D.K., M.F.F., P.B.L.H., A.E., A.B.G., and R.J.U. are employees of AstraZeneca. M.So. and D.D.A. were employees of AstraZeneca during duration of the study. All the authors declare no conflict of interest regarding publication of this study.

Acknowledgements

The project was funded by AstraZeneca. M.So. and D.D.A. were postdoctoral fellows sponsored by AstraZeneca Post Doc programme. We thank Drs Nick Oakes, Udo Bauer, Gerhard Böttcher, Ann-Cathrine Jönsson-Rylander (AstraZeneca, Sweden), Joanne Marks, Anselm Zdebik, Edward Debnam (University College London, UK) and Dr. Helen Cox (King's College London, UK) for scientific input and discussions and Dr. Fiona Gribble (University of Cambridge, UK) for sharing the *SGLT3* RNA-Seq data. We thank Rosie Perkins (Wallenberg Laboratory, Institute of Medicine, University of Gothenburg, Sweden) for an excellent editorial help. We acknowledge Drs Anne-Christine Andréasson, Maria Wigstrand, Ann Kjellstedt, Lena William-Olsson, Ulrika Johansson, Ulrika Dahlqvist, Maria Wågberg, Margareta Behrendt, Alba Carreras, Marcin Buler (AstraZeneca, Sweden) and Pavlína Kvapilová (Institute of Physiology, Czech Academy of Sciences, Czech Republic) for help throughout the experiments, sample collection or data retrieval and analyses.

E.B. is supported by the Wallenberg Centre for Molecular & Translational Medicine at University of Gothenburg and Knut and Alice Wallenberg Foundation, the Swedish Research Council (#2016/82), the Swedish Society for Medical Research (#S150086), Åke Wiberg Foundation (#M15-0058), and an ERC Starting Grant (#804418). V.W. is supported by Region Västra Götaland, Sweden (#ALFGGB-813871).

Appendix A. Supplementary data

Supplementary data to this article can be found online at <https://doi.org/10.1016/j.lfs.2020.118974>.

References

- [1] M. Ng, T. Fleming, M. Robinson, B. Thomson, N. Graetz, C. Margono, E.C. Mullany, S. Biryukov, C. Abbafati, S.F. Abera, J.P. Abraham, N.M.E. Abu-Rmeileh, T. Achoki,

- F.S. AlBuhairan, Z.A. Alemu, R. Alfonso, M.K. Ali, R. Ali, N.A. Guzman, W. Ammar, P. Anwari, A. Banerjee, S. Barquera, S. Basu, D.A. Bennett, Z. Bhutta, J. Blore, N. Cabral, I.C. Nonato, J.-C. Chang, R. Chowdhury, K.J. Courville, M.H. Criqui, D. K. Cundiff, K.C. Dabhadkar, L. Dandona, A. Davis, A. Dayama, S.D. Dharmaratne, E.L. Ding, A.M. Durrani, A. Esteghamati, F. Farzadfar, D.F.J. Fay, V.L. Feigin, A. Flaxman, M.H. Forouzanfar, A. Goto, M.A. Green, R. Gupta, N. Hafezi-Nejad, G. J. Skirbekk, H.C. Harewood, R. Havmoeller, S. Hay, L. Hernandez, A. Husseini, B. T. Idrisov, N. Ikeda, F. Islami, E. Jahangir, S.K. Jassal, S.H. Jee, M. Jeffreys, J. B. Jonas, E.K. Kabagambe, S.E.A.H. Khalifa, A.P. Kengne, Y.S. Khader, Y.-H. Khang, D. Kim, R.W. Kimokoti, J.M. Kinge, Y. Kokubo, S. Kosen, G. Kwan, T. Lai, M. Leinsalu, Y. Li, X. Liang, S. Liu, G. Logroscino, P.A. Lotufo, Y. Lu, J. Ma, N. K. Mainoo, G.A. Mensah, T.R. Merriman, A.H. Mokdad, J. Moschandreas, M. Naghavi, A. Naheed, D. Nand, K.M.V. Narayan, E.L. Nelson, M.L. Neuhouser, M. I. Nisar, T. Ohkubo, S.O. Oti, A. Pedroza, D. Prabhakaran, N. Roy, U. Sampson, H. Seo, S.G. Sepanlou, K. Shibuya, R. Shiri, I. Shue, G.M. Singh, J.A. Singh, V. Skirbekk, N.J.C. Stapelberg, L. Sturua, B.L. Sykes, M. Tobias, B.X. Tran, L. Trasande, H. Toyoshima, S. van de Vijver, T.J. Vasankari, J.L. Veerman, G. Velasquez-Melendez, V.V. Vlassov, S.E. Vollset, T. Vos, C. Wang, X. Wang, E. Weiderpass, A. Werdecker, J.L. Wright, Y.C. Yang, H. Yatsuya, J. Yoon, S.-J. Yoon, Y. Zhao, M. Zhou, S. Zhu, A.D. Lopez, C.J.L. Murray, E. Gakidou, Global, regional, and national prevalence of overweight and obesity in children and adults during 1980–2013: a systematic analysis for the Global Burden of Disease Study 2013, *Lancet* 384 (2014) 766–781, [https://doi.org/10.1016/S0140-6736\(14\)60460-8](https://doi.org/10.1016/S0140-6736(14)60460-8).
- [2] J. Dyer, I.S. Wood, A. Palejwala, A. Ellis, S.P. Shirazi-Beechey, Expression of monosaccharide transporters in intestine of diabetic humans, *Am. J. Physiol. Liver Physiol.* 282 (2002) G241–G248, <https://doi.org/10.1152/ajpgi.00310.2001>.
- [3] S.S. Thazhath, T. Wu, R.L. Young, M. Horowitz, C.K. Rayner, Glucose absorption in small intestinal diseases, *Expert Rev. Gastroenterol. Hepatol.* 8 (2014) 301–312, <https://doi.org/10.1586/17474124.2014.887439>.
- [4] H. Koepsell, The Na⁺-D-glucose cotransporters SGLT1 and SGLT2 are targets for the treatment of diabetes and cancer, *Pharmacol. Ther.* 170 (2017) 148–165, <https://doi.org/10.1016/j.pharmthera.2016.10.017>.
- [5] J.P. Wilding, Combination therapy for obesity, *J. Psychopharmacol.* 31 (2017) 1503–1508, <https://doi.org/10.1177/0269881117737401>.
- [6] A.J. Scheen, Sodium–glucose cotransporter type 2 inhibitors for the treatment of type 2 diabetes mellitus, *Nat. Rev. Endocrinol.* 16 (2020) 556–577, <https://doi.org/10.1038/s41574-020-0392-2>.
- [7] B. Zinman, C. Wanner, J.M. Lachin, D. Fitchett, E. Bluhmki, S. Hantel, M. Mattheus, T. Devins, O.E. Johansen, H.J. Woerle, U.C. Broedl, S.E. Inzucchi, Empagliflozin, cardiovascular outcomes, and mortality in type 2 diabetes, *N. Engl. J. Med.* 373 (2015) 2117–2128, <https://doi.org/10.1056/NEJMoa1504720>.
- [8] V. Perkovic, M.J. Jardine, B. Neal, S. Bompoint, H.J.L. Heerspink, D.M. Charytan, R. Edwards, R. Agarwal, G. Bakris, S. Bull, C.P. Cannon, G. Capuano, P.-L. Chu, D. de Zeeuw, T. Greene, A. Levin, C. Pollock, D.C. Wheeler, Y. Yavin, H. Zhang, B. Zinman, G. Meininger, B.M. Brenner, K.W. Mahaffey, CREDESCENCE Trial Investigators, Canagliflozin and renal outcomes in type 2 diabetes and nephropathy, *N. Engl. J. Med.* 380 (2019) 2295–2306, <https://doi.org/10.1056/NEJMoa1811744>.
- [9] V. Gorboulev, A. Schürmann, V. Vallon, H. Kipp, A. Jaschke, D. Klessen, A. Friedrich, S. Scherneck, T. Rieg, R. Cunard, M. Veyhl-Wichmann, A. Srinivasan, D. Balen, D. Breljak, R. Rexhepaj, H.E. Parker, F.M. Gribble, F. Reimann, F. Lang, S. Wiese, I. Sabolic, M. Sendtner, H. Koepsell, Na(+)-D-glucose cotransporter SGLT1 is pivotal for intestinal glucose absorption and glucose-dependent incretin secretion, *Diabetes*. 61 (2012) 187–196, <https://doi.org/10.2337/db11-1029>.
- [10] N.Q. Nguyen, T.L. Debrececi, J.E. Bambrick, B. Chia, J. Wishart, A.M. Deane, C. K. Rayner, M. Horowitz, R.L. Young, Accelerated intestinal glucose absorption in morbidly obese humans: relationship to glucose transporters, incretin hormones, and glycemia, *J. Clin. Endocrinol. Metab.* 100 (2015) 968–976, <https://doi.org/10.1210/jc.2014-3144>.
- [11] J.A. Dominguez Rieg, V.R. Chirasani, H. Koepsell, S. Senapati, S.K. Mahata, T. Rieg, Regulation of intestinal SGLT1 by catestatin in hyperleptinemic type 2 diabetic mice, *Lab. Invest.* 96 (2016) 98–111, <https://doi.org/10.1038/labinvest.2015.129>.
- [12] J.A. Dominguez Rieg, T. Rieg, What does sodium-glucose co-transporter 1 inhibition add: prospects for dual inhibition, *Diabetes. Obes. Metab.* 21 (2019) 43–52, <https://doi.org/10.1111/dom.13630>.
- [13] B. Mackenzie, M. Panayotova-Heiermann, D.D. Loo, J.E. Lever, E.M. Wright, SAAT1 is a low affinity Na⁺/glucose cotransporter and not an amino acid transporter. A reinterpretation, *J. Biol. Chem.* 269 (1994) 22488–22491.
- [14] M.A. Hediger, Y. Kanai, G. You, S. Nussberger, Mammalian ion-coupled solute transporters, *J. Physiol.* 482 (1995) 7–17, <https://doi.org/10.1113/jphysiol.1995.sp020559>.
- [15] M. Soták, J. Marks, R.J. Unwin, Putative tissue location and function of the SLC5 family member SGLT3, *Exp. Physiol.* 102 (2017) 5–13, <https://doi.org/10.1113/EP086042>.
- [16] A. Diez-Sampedro, B.A. Hirayama, C. Osswald, V. Gorboulev, K. Baumgarten, C. Volk, E.M. Wright, H. Koepsell, A glucose sensor hiding in a family of transporters, *Proc. Natl. Acad. Sci. U. S. A.* 100 (2003) 11753–11758, <https://doi.org/10.1073/pnas.1733027100>.
- [17] F. Delaere, A. Duchamp, L. Mounien, P. Seyer, C. Duraffourd, C. Zitoun, B. Thorens, G. Mithieux, The role of sodium-coupled glucose co-transporter 3 in the satiety effect of portal glucose sensing, *Mol. Metab.* 2 (2013) 47–53, <https://doi.org/10.1016/j.molmet.2012.11.003>.

- [18] A. Pal, D.B. Rhoads, A. Tavakkoli, Foregut exclusion disrupts intestinal glucose sensing and alters portal nutrient and hormonal milieu, *Diabetes* 64 (2015) 1941–1950, <https://doi.org/10.2337/db14-1578>.
- [19] R.K. Kothinti, A.B. Blodgett, P.E. North, R.J. Roman, N.M. Tabatabai, A novel SGLT is expressed in the human kidney, *Eur. J. Pharmacol.* 690 (2012) 77–83, <https://doi.org/10.1016/j.ejphar.2012.06.033>.
- [20] E.Y. Lee, S. Kaneko, P. Jutabha, X. Zhang, S. Seino, T. Jomori, N. Anzai, T. Miki, Distinct action of the α -glucosidase inhibitor miglitol on SGLT3, enteroendocrine cells, and GLP1 secretion, *J. Endocrinol.* 224 (2015) 205–214, <https://doi.org/10.1530/JOE-14-0555>.
- [21] S. Barcelona, D. Menegaz, A. Díez-Sampedro, Mouse SGLT3a generates proton-activated currents but does not transport sugar, *Am. J. Physiol. Cell Physiol.* 302 (2012) C1073–C1082, <https://doi.org/10.1152/ajpcell.00436.2011>.
- [22] T. Zietek, E. Rath, D. Haller, H. Daniel, Intestinal organoids for assessing nutrient transport, sensing and incretin secretion, *Sci. Rep.* 5 (2015), 16831, <https://doi.org/10.1038/srep16831>.
- [23] T. Sato, R.G. Vries, H.J. Snippet, M. van de Wetering, N. Barker, D.E. Stange, J. H. Van Es, A. Abo, P. Kujala, P.J. Peters, H. Clevers, Single Lgr5 stem cells build crypt-villus structures in vitro without a mesenchymal niche, *Nature* 459 (2009) 262–265, <https://doi.org/10.1038/nature07935>.
- [24] T. Sato, D.E. Stange, M. Ferrante, R.G.J.J. Vries, J.H. Van Es, S. Van Den Brink, W. J. Van Houdt, A. Pronk, J. Van Gorp, P.D. Siersema, H. Clevers, Long-term expansion of epithelial organoids from human colon, adenoma, adenocarcinoma, and Barrett's epithelium, *Gastroenterology* 141 (2011) 1762–1772, <https://doi.org/10.1053/j.gastro.2011.07.050>.
- [25] J.P. Stoehr, J.E. Byers, S.M. Clee, H. Lan, I.V. Boronenkov, K.L. Schueler, B. S. Yandell, A.D. Attie, Identification of major quantitative trait loci controlling body weight variation in ob/ob mice, *Diabetes* 53 (2004) 245–249, <https://doi.org/10.2337/diabetes.53.1.245>.
- [26] K.M. Vincent, J.W. Sharp, H.E. Raybould, Intestinal glucose-induced calcium-calmodulin kinase signaling in the gut-brain axis in awake rats, *Neurogastroenterol. Motil.* 23 (2011) e282–e293, <https://doi.org/10.1111/j.1365-2982.2011.01673.x>.
- [27] A.M. Habib, P. Richards, L.S. Cairns, G.J. Rogers, C.A.M. Bannon, H.E. Parker, T.C. E. Morley, G.S.H. Yeo, F. Reimann, F.M. Gribble, Overlap of endocrine hormone expression in the mouse intestine revealed by transcriptional profiling and flow cytometry, *Endocrinology* 153 (2012) 3054–3065, <https://doi.org/10.1210/en.2011-2170>.
- [28] G.P. Roberts, P. Larraufie, P. Richards, R.G. Kay, S.G. Galvin, E.L. Miedzybrodzka, A. Leiter, H.J. Li, L.L. Glass, M.K.L. Ma, B. Lam, G.S.H. Yeo, R. Scharfmann, D. Chiarugi, R.H. Hardwick, F. Reimann, F.M. Gribble, Comparison of human and murine enteroendocrine cells by transcriptomic and peptidomic profiling, *Diabetes* 68 (2019) 1062–1072, <https://doi.org/10.2337/db18-0883>.
- [29] P. O'Brien, C.P. Corpe, Acute effects of sugars and artificial sweeteners on small intestinal sugar transport: a study using CaCo-2 cells as an in vitro model of the human enterocyte, *PLoS One* 11 (2016), e0167785, <https://doi.org/10.1371/journal.pone.0167785>.
- [30] R.E. McConnell, A.E. Benesh, S. Mao, D.L. Tabb, M.J. Tyska, Proteomic analysis of the enterocyte brush border, *Am. J. Physiol. Gastrointest. Liver Physiol.* 300 (2011) G914–G926, <https://doi.org/10.1152/ajpgi.00005.2011>.
- [31] A. Díez-Sampedro, S. Barcelona, Sugar binding residue affects apparent Na⁺ affinity and transport stoichiometry in mouse sodium/glucose cotransporter type 3B, *J. Biol. Chem.* 286 (2011) 7975–7982, <https://doi.org/10.1074/jbc.M110.187880>.
- [32] A.A. Voss, A. Díez-Sampedro, B.A. Hirayama, D.D.F. Loo, E.M. Wright, Imino sugars are potent agonists of the human glucose sensor SGLT3, *Mol. Pharmacol.* 71 (2007) 628–634, <https://doi.org/10.1124/mol.106.030288>.
- [33] Y.-G.G. Li, D.-F.F. Ji, S. Zhong, T.-B.B. Lin, Z.-Q.Q. Lv, G.-Y.Y. Hu, X. Wang, 1-deoxyxojirimycin inhibits glucose absorption and accelerates glucose metabolism in streptozotocin-induced diabetic mice, *Sci. Rep.* 3 (2013), 1377, <https://doi.org/10.1038/srep01377>.
- [34] F.M. Gribble, L. Williams, A.K. Simpson, F. Reimann, A novel glucose-sensing mechanism contributing to glucagon-like peptide-1 secretion from the GLUTag cell line, *Diabetes* 52 (2003) 1147–1154, <https://doi.org/10.2337/diabetes.52.5.1147>.
- [35] E.W. Sun, D. de Fontgalland, P. Rabbitt, P. Hollington, L. Sposato, S.L. Due, D. A. Wattoo, C.K. Rayner, A.M. Deane, R.L. Young, D.J. Keating, Mechanisms controlling glucose-induced GLP-1 secretion in human small intestine, *Diabetes* 66 (2017) 2144–2149, <https://doi.org/10.2337/db17-0058>.
- [36] S.L. Freeman, D. Bohan, N. Darcel, H.E. Raybould, Luminal glucose sensing in the rat intestine has characteristics of a sodium-glucose cotransporter, *Am. J. Physiol. Gastrointest. Liver Physiol.* 291 (2006) G439–G445, <https://doi.org/10.1152/ajpgi.00079.2006>.
- [37] J. Fahrenkrug, O.B. Schaffalitzky de Muckadell, Plasma secretin concentration in man: effect of intraduodenal glucose, fat, amino acids, ethanol, HCl, or ingestion of a meal, *Eur. J. Clin. Invest.* 7 (1977) 201–203, <https://doi.org/10.1111/j.1365-2362.1977.tb01598.x>.
- [38] H. Koepsell, Glucose transporters in the small intestine in health and disease, *Pflügers Arch.* 472 (2020) 1207–1248, <https://doi.org/10.1007/s00424-020-02439-5>.
- [39] C. Fanjul, J. Barrenetxe, C. Iñigo, Y. Sakar, R. Ducroc, A. Barber, M.P. Lostao, Leptin regulates sugar and amino acids transport in the human intestinal cell line Caco-2, *Acta Physiol. (Oxf)* 205 (2012) 82–91, <https://doi.org/10.1111/j.1748-1716.2012.02412.x>.
- [40] C. Weidinger, J.F. Ziegler, M. Letizia, F. Schmidt, B. Siegmund, Adipokines and their role in intestinal inflammation, *Front. Immunol.* 9 (2018) 1974, <https://doi.org/10.3389/fimmu.2018.01974>.
- [41] B.K. Wölnerhanssen, A.W. Moran, G. Burdyga, A.C. Meyer-Gerspach, R. Peterli, M. Manz, M. Thumshirn, K. Daly, C. Beglinger, S.P. Shirazi-Beechey, Deregulation of transcription factors controlling intestinal epithelial cell differentiation; a predisposing factor for reduced enteroendocrine cell number in morbidly obese individuals, *Sci. Rep.* 7 (2017), 8174, <https://doi.org/10.1038/s41598-017-08487-9>.
- [42] J.J. Holst, Enteroendocrine secretion of gut hormones in diabetes, obesity and after bariatric surgery, *Curr. Opin. Pharmacol.* 13 (2013) 983–988, <https://doi.org/10.1016/j.coph.2013.09.014>.
- [43] J.-B. Cavin, A. Couvelard, R. Lebtahi, R. Ducroc, K. Arapis, E. Voittellier, F. Cluzeaud, L. Gillard, M. Hourseau, N. Mikail, L. Ribeiro-Parenti, N. Kapel, J.-P. Marmuse, A. Bado, M. Le Gall, Differences in alimentary glucose absorption and intestinal disposal of blood glucose after Roux-en-Y gastric bypass vs sleeve gastrectomy, *Gastroenterology* 150 (2016) 454–464.e9, <https://doi.org/10.1053/j.gastro.2015.10.009>.
- [44] H.Y. Bhutta, T.E. Deelman, C.W. le Roux, S.W. Ashley, D.B. Rhoads, A. Tavakkoli, Intestinal sweet-sensing pathways and metabolic changes after Roux-en-Y gastric bypass surgery, *Am. J. Physiol. Gastrointest. Liver Physiol.* 307 (2014) G588–G593, <https://doi.org/10.1152/ajpgi.00405.2013>.
- [45] K. Ahmed, N. Penney, A. Darzi, S. Purkayastha, Taste changes after bariatric surgery: a systematic review, *Obes. Surg.* 28 (2018) 3321–3332, <https://doi.org/10.1007/s11695-018-3420-8>.
- [46] Y. Ren, Z. Zhao, G. Zhao, Q. Liu, Z. Wang, R. Liu, Sleeve gastrectomy surgery improves glucose metabolism by downregulating the intestinal expression of sodium–glucose cotransporter-3, *J. Investig. Surg.* 0 (2020) 1–9, <https://doi.org/10.1080/08941939.2020.1810370>.
- [47] A.T. Stearns, A. Balakrishnan, A. Tavakkolizadeh, Impact of Roux-en-Y gastric bypass surgery on rat intestinal glucose transport, *AJP Gastrointest. Liver Physiol.* 297 (2009) G950–G957, <https://doi.org/10.1152/ajpgi.00253.2009>.
- [48] M.B. Mumphy, Z. Hao, R.L. Townsend, L.M. Patterson, H.-R. Berthoud, Sleeve gastrectomy does not cause hypertrophy and reprogramming of intestinal glucose metabolism in rats, *Obes. Surg.* 25 (2015) 1468–1473, <https://doi.org/10.1007/s11695-014-1547-9>.
- [49] J.-B. Cavin, A. Bado, M. Le Gall, Intestinal adaptations after bariatric surgery: consequences on glucose homeostasis, *Trends Endocrinol. Metab.* (2017), <https://doi.org/10.1016/j.tem.2017.01.002>.
- [50] J.D. Douros, J. Tong, D.A. D'Alessio, The effects of bariatric surgery on islet function, insulin secretion, and glucose control, *Endocr. Rev.* 40 (2019) 1394–1423, <https://doi.org/10.1210/er.2018-00183>.
- [51] R.C. Moffett, N.G. Docherty, C.W. le Roux, The altered enteroendocrine repertoire following roux-en-Y-gastric bypass as an effector of weight loss and improved glycaemic control, *Appetite* 156 (2021), 104807, <https://doi.org/10.1016/j.appet.2020.104807>.
- [52] P. O'Brien, R. Hewett, C. Corpe, Sugar sensor genes in the murine gastrointestinal tract display a cephalocaudal axis of expression and a diurnal rhythm, *Physiol. Genomics* 50 (2018) 448–458, <https://doi.org/10.1152/physiolgenomics.00139.2017>.
- [53] M. Soták, J. Bryndová, P. Ergan, K. Vagnerová, P. Kvapilová, M. Vodička, J. Pácha, A. Sumová, Peripheral circadian clocks are diversely affected by adrenalectomy, *Chronobiol. Int.* 33 (2016) 520–529, <https://doi.org/10.3109/07420528.2016.1161643>.
- [54] A. Tavakkolizadeh, U.V. Berger, K.R. Shen, L.L. Levitsky, M.J. Zinner, M. A. Hediger, S.W. Ashley, E.E. Whang, D.B. Rhoads, Diurnal rhythmicity in intestinal SGLT-1 function, V(max), and mRNA expression topography, *Am. J. Physiol. Gastrointest. Liver Physiol.* 280 (2001) G209–G215.
- [55] M. Soták, L. Polidarová, J. Muslíková, M. Hock, A. Sumová, J. Pácha, Circadian regulation of electrolyte absorption in the rat colon, *Am. J. Physiol. Gastrointest. Liver Physiol.* 301 (2011) G1066–G1074, <https://doi.org/10.1152/ajpgi.00256.2011>.
- [56] H. Ando, M. Kumazaki, Y. Motosugi, K. Ushijima, T. Maekawa, E. Ishikawa, A. Fujimura, Impairment of peripheral circadian clocks precedes metabolic abnormalities in ob/ob mice, *Endocrinology* 152 (2011) 1347–1354, <https://doi.org/10.1210/en.2010-1068>.
- [57] M. Gil-Lozano, W.K. Wu, A. Martchenko, P.L. Brubaker, High-fat diet and palmitate alter the rhythmic secretion of glucagon-like peptide-1 by the rodent L-cell, *Endocrinology* 157 (2016) 586–599, <https://doi.org/10.1210/en.2015-1732>.
- [58] A.T. Stearns, A. Balakrishnan, D.B. Rhoads, S.W. Ashley, A. Tavakkolizadeh, Diurnal expression of the rat intestinal sodium-glucose cotransporter 1 (SGLT1) is independent of local luminal factors, *Surgery* 145 (2009) 294–302, <https://doi.org/10.1016/j.surg.2008.11.004>.
- [59] D.D. Aidingupu, S.O. Göpel, J. Grönros, M. Behrendt, M. Soták, T. Miliotis, U. Dahlqvist, L.-M. Gan, A.-C. Jönsson-Rylander, SGLT2 inhibition with empagliflozin improves coronary microvascular function and cardiac contractility in prediabetic ob/ob^{-/-} mice, *Cardiovasc. Diabetol.* 18 (2019), 16, <https://doi.org/10.1186/s12933-019-0820-6>.
- [60] C. Kless, V.M. Müller, V.L. Schüppel, M. Lichtenegger, M. Rychlik, H. Daniel, M. Klingenspor, D. Haller, Diet-induced obesity causes metabolic impairment independent of alterations in gut barrier integrity, *Mol. Nutr. Food Res.* 59 (2015) 968–978, <https://doi.org/10.1002/mnfr.201400840>.
- [61] E. Rath, E. Berger, A. Messlik, T. Nunes, B. Liu, S.C. Kim, N. Hoogenraad, M. Sans, R.B. Sartor, D. Haller, Induction of dsRNA-activated protein kinase links mitochondrial unfolded protein response to the pathogenesis of intestinal

- inflammation, *Gut* 61 (2012) 1269–1278, <https://doi.org/10.1136/gutjnl-2011-300767>.
- [62] T. Zietek, E. Rath, Intestinal organoids, in: J. Davies, M. Lawrence (Eds.), *Organs and Organoids*, Academic Press, 2018, pp. 43–71, <https://doi.org/10.1016/B978-0-12-812636-3.00003-1>.
- [63] A. Casselbrant, J.M. Söfteland, M. Hellström, M. Malinauskas, M. Oltean, Luminal polyethylene glycol alleviates intestinal preservation injury irrespective of molecular size, *J. Pharmacol. Exp. Ther.* 366 (2018) 29–36, <https://doi.org/10.1124/jpet.117.247023>.